MODELING THE GEOMETRY OF A MINERAL DEPOSIT DOMAIN WITH A POTENTIAL FIELD

Didier Renard [1], Laurent Wagner [2], Jean-Paul Chilès [3], Jacques Deraisme [4], Rudi Jahoda[5] and John Vann[6]

[1] Centre of Geosciences and Geoengineering, MINES ParisTech, 35 rue Saint-Honoré, 77305 Fontainebleau, France, phone: +33 1 64 69 47 80, email: didier.renard@mines-paristech.fr

[2] Geovariances, 49bis avenue Franklin Roosevelt, 77215 Avon, France,
phone: +33 1 60 74 90 90, email: wagner@geovariances.com

[3] Centre of Geosciences and Geoengineering, MINES ParisTech, 35 rue Saint-Honoré, 77305 Fontainebleau, France, phone: +33 1 64 69 47 86, email: jean-paul.chiles@mines-paristech.fr

[4] Geovariances, 49bis avenue Franklin Roosevelt, 77215 Avon, France,
phone: +33 1 60 74 90 90, email: deraisme@geovariances.com

[5] Geology Manager – La Colosa, AngloGold Ashanti, Edif Banco de La República,Ibagué, Tolima, Colombia, email : rjahoda@AngloGoldAshanti.com.

[6] Vice President Mineral Resources, Anglogold Ashanti, 44 St. Georges Terrace, Perth, WA, 6000, Australia, email : jvann@AngloGoldAshanti.com.

SUMMARY. The potential field method, successfully used in geological mapping applications, has been developed here in the context of mineral deposit modeling, where in comparison to geological mapping we have many drill holes but usually few structural data.

The principle of the method is to derive the geometry of the domain under study from a 3D interpolation of a scalar field, known as the potential field. This is achieved by cokriging from information on contacts from drill holes and on structural data linked with the gradient of the potential field. Even so the amount of information brought by the drill holes is much larger than just the transitions from outside to inside the domain (or the reverse). Soft information is efficiently added to the hard contact data by means of control points processed with the Gibbs sampler algorithm.The potential field approach provides by-products such as the cokriging variance, and the gradient of the estimated potential field, which can be turned into an uncertainty measure on the location of the domain boundary or used to map the probability to be within the given domain.

The proposed potential field method is put into practice in a case study of a gold porphyry deposit, La Colosa in the Central Cordillera of Colombia. Hardness measurements related to lithology and alteration have been collected on exploration drill-cores using the Equotip hardness tester. After simple pre-processing of this data, one domain has been modeled and probability map has been calculated.

INTRODUCTION

The main characteristics of mineral deposit are the ore tonnage and the average grade of its various ore types or domains. Once the geometry of a domain is known, its grade can be estimated with 3D geostatistical tools providing a block model and/or a global estimation, both with an attached uncertainty in the form of an estimation variance. The geometry of a domain, thus its ore tonnage, is sometimes an easy question. For example, if the domain is a sedimentary layer, it is delimited by a foot wall and a hanging wall, whose elevations (or depths) can be studied with 2D geostatistics. An alternative is to simply consider the mineralization thickness and to study the grade through the accumulation (i.e., the product of a thickness and a grade, which has dimensions of 'metal'). Accumulation approaches are in 2D and cannot handle complex 3D geometries, in such cases 3D models often based on cross section interpretations are used. These 3D models are deterministic, in other words they are without specification of uncertainty.

The uncertainty on geometric models can be very large and it is now widely appreciated that this should be addressed. An answer is provided by the so-called transitive methods (see Renard et al., 2013) but this answer is global and, for example, cannot provide simulations of the geometry. We investigate here another approach, that of potential fields. It was first developed for 3D geological mapping (Calcagno et al., 2008). We develop it here in the different context of mining evaluation.

METHODOLOGY

Principle of the Potential Field Method

The potential field method is designed to model interfaces between two volumes when the following types of data are available:

 1. Points located on the interfaces; and

2. Structural data defining planes supposed to be locally sub-parallel to the interfaces.

In 3D modeling of a sedimentary geological interface, the structural data are unit vectors orthogonal to the main planar geological anisotropy (e.g. bedding, schistosity, or foliation) and pointing towards the direction of younger formations. In 3D modeling of a mineralization domain, they are unit vectors pointing from the inside to the outside of the domain.

The basic method (Lajaunie et al., 1997) is designed to model a single interface. The principle is to define a *potential field*, namely a scalar function $T(x)$ of location x in 3D space, such that the geological interface corresponds to an isopotential surface, that is, the set of points x that satisfy $T(x) = c,$ a given constant value (a *level set*). In the case of the example above, T could be interpreted as geological time, or an increasing function of time, and the interface as an isochron surface. This figurative interpretation can be adequate in some applications but is not necessary for the development of the method.

The data are interpreted as follows:

1. *Interface Points:* The potential value *c* associated with the interface is not known but the potential difference between two points of the interface is equal to zero (since it is a surface of equipotential). If we denote by $x_\alpha : \alpha = 1, \ldots, M+1$, the points know to belong to the interface, they are translated into *M* increments $T(x_{\alpha+1}) - T(x_\alpha) = 0 : \alpha = 1, \ldots, M$.

2. *Orientation Data:* Let us denote by $x_\beta : \beta = 1, \ldots, N$, the location of the orientation data (they are not necessarily located on the interface and thus in general do not coincide with the set of points x_α). These data are polarized unit vectors that are interpreted as the gradient of the potential field. They provide the values at points x_β of the three partial derivatives $\partial T / \partial u_1$, $\partial T / \partial u_2$, and $\partial T / \partial u_3$, where u_1, u_2, u_3 denote the axes directions in the 3D space.

T itself is defined up to an arbitrary constant taken to be the potential at an arbitrary reference point x_0. We estimate a potential difference using a cokriging estimator of the form

$$T^*(x) - T^*(x_0) = \sum_{\alpha=1}^{M} \lambda_\alpha \left[T(x_{\alpha+1}) - T(x_\alpha) \right] + \sum_{\beta=1}^{N} \sum_{i=1}^{3} \nu_{\beta i} \, \frac{\partial T}{\partial u_i}(x_\beta)$$

where λ_α and $\nu_{\beta i}$ are the cokriging weights attached to the data. The intriguing feature of this approach is that it permits a modeling of the interface using only potential differences equal to zero and gradients. The potential increments have a zero value but their presence in the estimator causes the weights on the gradient to be different from what they would be based on the gradient data alone. Conversely, in the absence of gradient data the cokriging estimator would be identically zero (note that a single gradient vector can be enough).

Interpolation of the Potential Field

T(x) is assumed to be a random function with a polynomial drift

$$m(x) = \sum_{\ell=0}^{L} b_\ell \, f^\ell(x)$$

and a stationary covariance *K(h)*. The $f^\ell(x)$ are basic drift functions (usually monomials) and the b_ℓ are their coefficients. Since the vertical direction usually can play a special role in stratified deposits, the degree of the polynomial drift can be higher vertically than horizontally and the covariance can be anisotropic. For example, if we model a sub-horizontal interface, it makes sense to assume a vertical linear drift. A domain with the shape of an ellipsoid would correspond to a quadratic drift, defined by the 10 monomials with degree less than or equal to 2 in the 3D space.

Once the basic functions of the drift *m(x)* and the covariance *K(h)* are known, we have all the ingredients to perform a cokriging in the presence of gradient data, as shown in Chilès and Delfiner (2012, Section 5.5.2). Indeed, the drifts of the partial derivatives are the partial derivatives of *m(x)*, the covariances of partial derivatives are second-order partial derivatives of

K, and the cross-covariances of the potential field and partial derivatives are partial derivatives of K.

To ensure the continuity of the estimates, cokriging is carried out in unique neighborhood. The kriging system has $M + 3N + L$ equations with as many unknowns: the $M + 3N$ weights and L Lagrange parameters (indeed the constant drift function $f^0(x) \equiv 1$ is eliminated from the cokriging system because we only consider increments). If we do not need the cokriging variance, the dual form of cokriging is used, which has two advantages:

1. The cokriging system is solved once for all; and

2. the dual form is especially well-suited when cokriging is considered as an interpolator, because the estimate at any desired point x is then a linear combination of the covariances between the target increment and the data. This property can be used to track the desired isosurface by plugging a gradient search algorithm on the potential field interpolator.

The choice of the covariance function is important. It cannot be determined from the interface points, because these only produce increments with a zero value. When many structural data are available, the variograms of the partial derivatives can be calculated. Because the variograms of partial derivatives are second-order derivatives of the variogram of the potential field, they give access to the variogram or covariance of the potential field. Because T is differentiable, K must be twice differentiable. A good candidate is thus the cubic covariance model because it has imposed spatial smoothness. Several studies at a regional scale have shown that a good fitting can be obtained with a sum of two or three anisotropic cubic covariance models (Aug, 2004).

Further Points

Data Points Inside or Outside the Domain: With the above notations, an inner point is characterized by $T(x) < c$, while an outer point is characterized by $T(x) > c$. If this kind of inequality is given at some control points (soft data), it can be taken into account with the Gibbs sampler (e.g., Chilès and Delfiner, 2012, section 7.6.3), provided that T is assumed to be Gaussian, which seems to be a reasonable assumption. The Gibbs sampler is an iterative procedure that replaces the soft data by simulated values conditional on the hard and soft data. By repeating the process and averaging the results we obtain the conditional expectation of the potential field at the soft data locations. These have then simply to be considered as true data in the cokriging process. We will see that this method is very useful for our applications.

Translating the Cokriging Variance into Geometric Uncertainty: Cokriging gives the estimation variance of $T(x) - T(x_0)$. Let us choose for x_0 a point located on the interface. Then we have

$$\Pr\{x \text{ inside the domain}\} = \Pr\{T(x) - T(x_0) < 0\} = \Pr\{T^*(x) - T^*(x_0) + U < 0\}$$

where U is the cokriging error. Denoting the cokriging variance by σ^2_{CK}, we then have

$$\Pr\{x \text{ inside the domain}\} = G\left(-\frac{T^*(x) - T^*(x_0)}{\sigma_{CK}}\right)$$

where *G* is the standard normal cumulative distribution function. This enables the translation of the cokriging variance map into a map of the probability to be inside the domain.

Conditional Simulation of the Domain: The conditional simulation of the potential field can be carried out with the usual techniques available for Gaussian random functions (Chilès and Delfiner, 2012, chapter 7). It is therefore possible to provide a set of equiprobable images of the domain geometry. This is also the way to model the uncertainty on the global volume.

Modeling Several Domains: If the domains are separated by sub-parallel interfaces, for example a layered or zones geological setting, the interfaces can be considered as distinct iso-surfaces (or level sets) of the same potential field. In the above expression of $T^*(x) - T^*(x_0)$ other terms similar to the first sum must be added. If the domains are independent, each one is modeled with a specific potential field.

Specificity of Mineral Deposit Domain Applications

The potential field approach has proven to be successful in 3D geological mapping applications at a regional scale. The standard situation uses a limited number of interface points and a large number of structural data, all observed on outcrops, possibly complemented by some drill hole data. In mining applications, the typical situation includes many drill hole data but few structural data (in the limiting case, we fix the gradient at a single point).

A consequence is that the inference of the covariance is heuristic and thus calls for techniques of trial and error and cross validation.

Another specificity is that many bore holes are barren and provide no interface point. It is nevertheless often necessary to include them through inequality data (Gibbs points), otherwise there is the risk that the modeled domain includes some part of these bore holes, which would not be consistent.

CASE STUDY

Geology

The La Colosa porphyry gold deposit is located in the central cordillera of Colombia, approximately 20km to the west of the city of Ibague and 150km to the west of the capital Bogota. The deposit consists of a polyphase Miocene (8-9Ma) magmatic complex intruded into shales and schists of the Phanerozoic Cajamarca Group (Vinasco et al. 2006). The location of the magmatic complex is related to a small pull-apart basin itself localised by NW-SE and NE-SW trending normal faults, which dip steeply between 70º and vertical.

The early intrusives are dioritic in composition, consisting of plagioclase phenocrysts set in a matrix consisting predominantly of plagioclase and hornblende. Four early diorite generations have been recognised on the basis of cross-cutting and brecciation relationships, texture,

phenocryst proportion and grain size. The early diorites occur as stocks form the core of the deposit.

Later intermineral diorites occur peripheral to, and intruding into, the early diorites. These form a large intrusive body in the north of the deposit, and also occur as a series of NW trending dykes (which do not outcrop) in the country rocks to the south of the intrusive complex. Three intermineral generations are recognised on the basis of cross-cutting relationships, texture and grain size, they are similar in composition to the early diorites.

The last stage of intrusive activity is defined by a granodioritic (locally termed dacite) stock to the east of the early diorites, and coeval NW trending dykes.

Country rocks of the Cajamarca Group consist of a sequence of dark green to black shales with a pre-existing penetrative cleavage related to earlier folding. These have been hornfelsed along intrusive contacts, especially to the south of the early diorite complex.

Alteration is complex, with multiple generations related to the different intrusive events. Mineralisation in the intrusives is best developed in the early diorites, where grades of >1g/t occur associated with sulphide-bearing veins within potassic and to a lesser extent phyllic alteration assemblages; disseminated mineralisation is also evident. Grades in the intermineral diorites tend to be lower at ~0.8g/t, and gold is again predominantly associated with sulphide veining. Grades in the late granodiorite are low (0.3-0.6g/t), indicating that the mineralisation system by this stage was decreasing in intensity. Higher grades are locally associated with the argillic alteration, suggesting that there may have been remobilisation of early mineralisation into faults. The hornfels is generally well mineralised, which is both disseminated and vein-associated, while mineralisation in the schists tends to be structurally controlled and areally more restricted.

The wide variety of both lithologies and alteration types has produced a wide range of primary rock hardness, which is evident from the variation seen in Equotip values
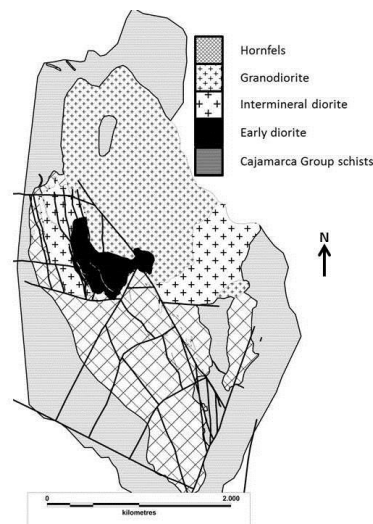
Figure 1: Simplified geological map showing the main lithologies.

6

Equotip Data Acquisition

The Equotip 3 is the third generation of a portable hardness tester manufactured by Proceq, a Swiss company. Originally designed primarily for metal testing, it has subsequently been used to test a wider range of materials including rock samples. Examples of application to rock hardness have been presented by Meulenkamp and Alvarez (1999) and Aoki and Matsukara (2008). A major advantage of Equotip over similar devices such as the Schmidt hammer is that Equotip operates at much lower energy, and so has low penetration (and consequently does not record information about the material on which the sample is tested), is non-destructive, and can be used on softer materials such as oxidized rock.

The Equotip comprises an impact body consisting of a spring-loaded spherical tip and a magnet, encased in a small plastic body containing a wire coil. This is linked to a control/data capture unit. During measurement, the spring-loaded tip is impacted against a sample and as the impact body rebounds the magnet generates an induction voltage as the impact body passes through the coil. The induction voltage is directly proportional to the rebound velocity. Data are captured as the Leeb rebound value for hardness L, where L = Rebound Velocity/Impact Velocity x 1000. Several different tip materials are available, for this work Type D (tungsten carbide) has been used.

Measurements were made exclusively on drill-core. The core was thoroughly cleaned and vacuumed prior to measurement to remove dust, and placed in a custom-built marble block to ensure consistency of measurement, and measurements were made on the centre-line of the core taking care to avoid any fractures that could influence the data. A measurement spacing of 2cm was used, corresponding to 100 measurements per 2m assay interval for intact core. Where core was highly fractured no data were collected, resulting in some cases in a lower number of measurements per assay interval.

The instrument was calibrated daily by collecting twenty measurements on standard test blocks supplied by the manufacturer, and these were then used to correct measurements for incorporation into the database. Where the calibration data were found to outside tolerance, the tip was replaced, and the instrument recalibrated prior to continuing with data collection. Measurements for each two-meter interval have been averaged to provide a single value, and in addition variance and percentile statistics have been calculated.

Data Pre-processing

Low hardness values can be generated if sulphide grains (for example) are measured, or if the measurement are too close to a fracture/crack. In order to remove those effects we have kept the 90th percentile of the N measurements in the assay interval. Figure 2 shows the distribution of the 32000 values of the 90th percentile of the 2-m long samples available along the 230 drill holes.
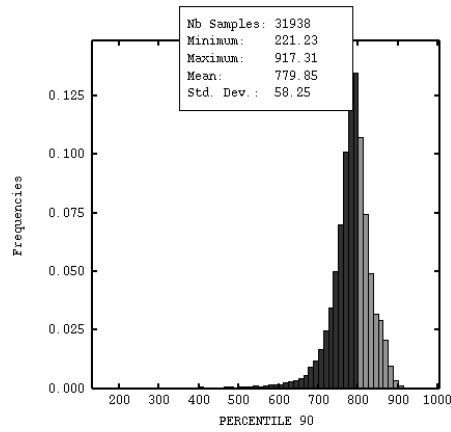
Figure 2: Histogram of the 90th Percentile of the Equotip data over a 2-m sample.

 The definition of a domain, which is linked to lithologies and alterations, was obtained by applying a threshold on this percentile. The value 800 corresponding to 35% of samples was chosen. The resulting indicator was then filtered to define intervals inside the domain and intervals outside the domain with a minimum length: small intervals inside, included in bigger intervals outside, are incorporated in the outside interval and vice versa. The points where the interval changes from inside to outside make the contacts input in the potential kriging algorithm (Figure 3).
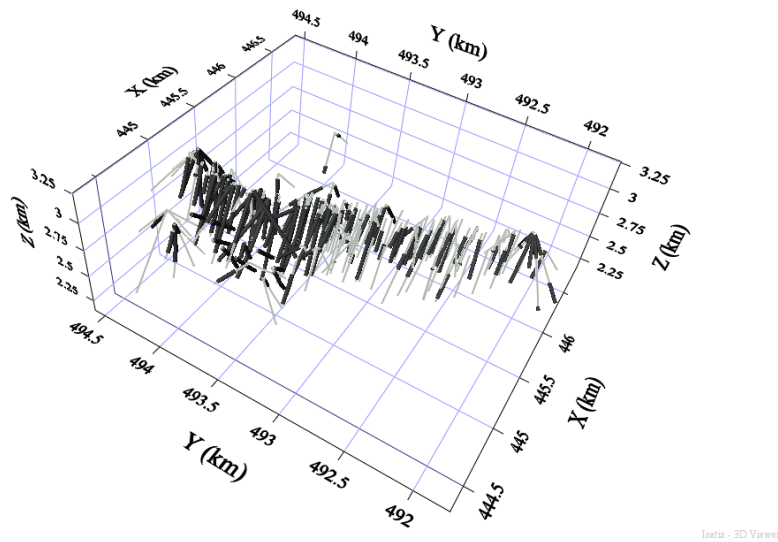
Figure 3: Perspective view of the drill holes layout with information of the domain intercepts.

Results

A first trial was made to model the domain, based on Equotip data as defined above, by adding a single gradient to the set of contact points. A stationary and anisotropic model was used (variogram with a dip of 15° and ranges of 350m, 700m, 300m), accounting for the elongation along OY of the orebody. The general shape of the resulting geometries is correctly represented but many drill hole with intercepts inside the domain are excluded from the modeled domain (see Figure 4), which results in a rather low volume.
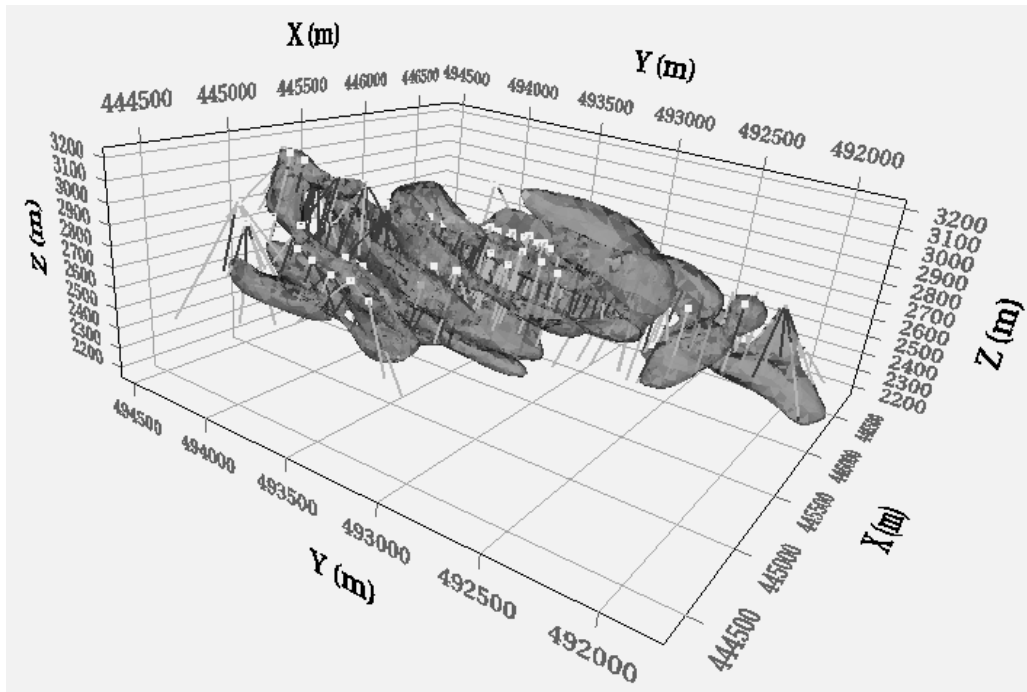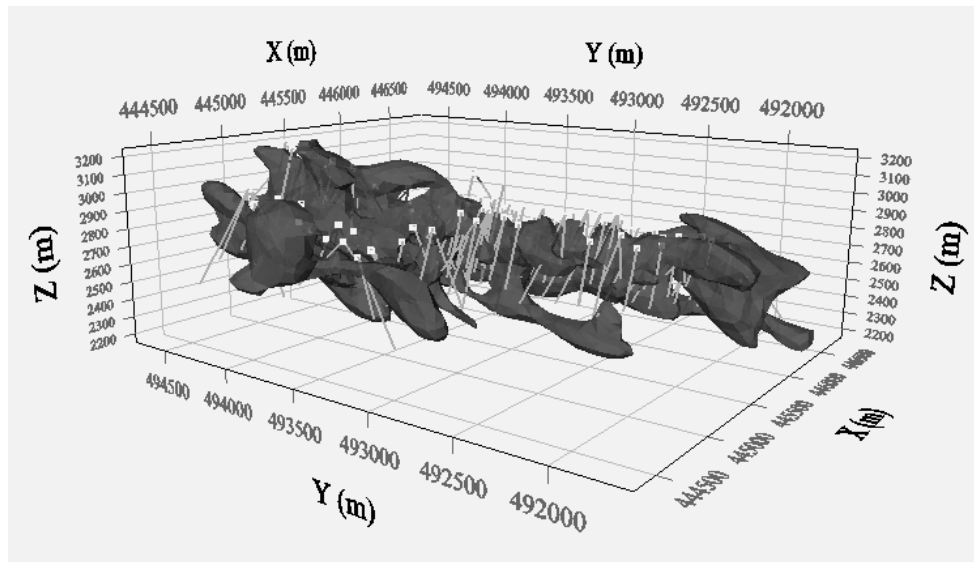

Figure 4: Domain obtained from Potential Kriging using contacts with drill holes and a single gradient.

In order to account for drill hole information beyond the contacts, a set of 460 Gibbs points have been added, that is, one per interval, an interval being a continuous pass entirely inside or outside the domain. The resulting domain looks more acceptable than previously with a significant increase of the volume. Some extra bodies (two can be seen in the bottom part and one at the top of Figure 5) appear without support from the drill hole data. Besides, looking in more details (not legible on a black and white figure) in the northern area more densely drilled, many intercepts of smaller length are not honored. This is not in contradiction with the data since the contacts are honored, it is just inverting the sense of the domain inclusion. By adding soft information within the intervals we attempt to remedy to these 'inversion problems'.
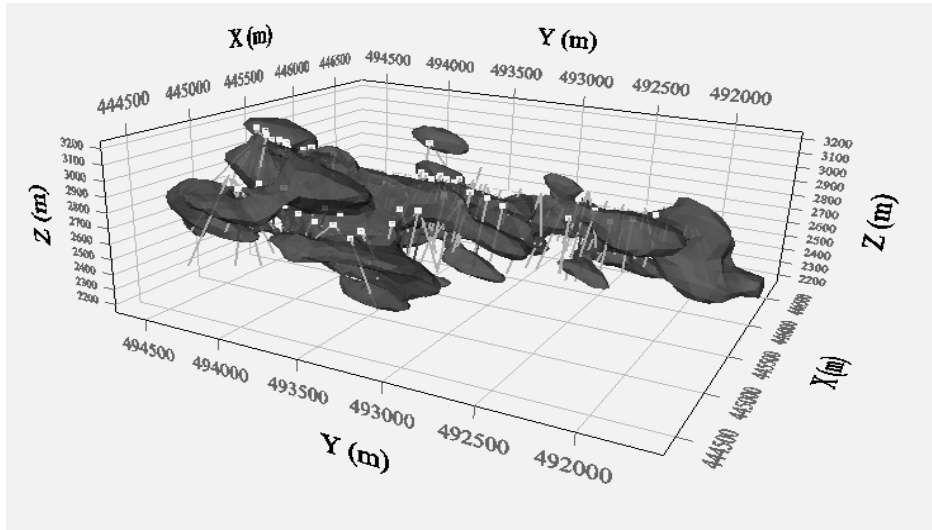
Figure 5: Domain obtained from Potential Kriging using contacts with drill holes, a single gradient and additional Gibbs points (one per interval).

The last attempt (Figure 6) has been made by adding more Gibbs points (600) with possibly more points within an interval if necessary. The choice of the Gibbs points to keep for modeling depends on the validation of QC points regularly put every 50m: if a QC points is not honored (status inside/outside the domain from drill hole information) it is transformed into a Gibbs point. The volume is about twice as large as in the first trial ($8Mm^3$ instead of $4.7Mm^3$).

Figure 6: Domain obtained from Potential Kriging using contacts with drill holes, a single gradient and additional Gibbs points (optimized number per interval).

The calculation of the probability to belong to the domain is illustrated on one section (Figure 7). Four classes of probability can be visualized with different greyscale colours. At the kriged domain boundary the probability is 0.5. When moving towards the domain interior the probability increases (between 0.5 and 0.55 pale grey, above 0.55 white), when moving towards the domain exterior the probability decreases (between 0.45 and 0.5 dark grey, less than 0.45 black).
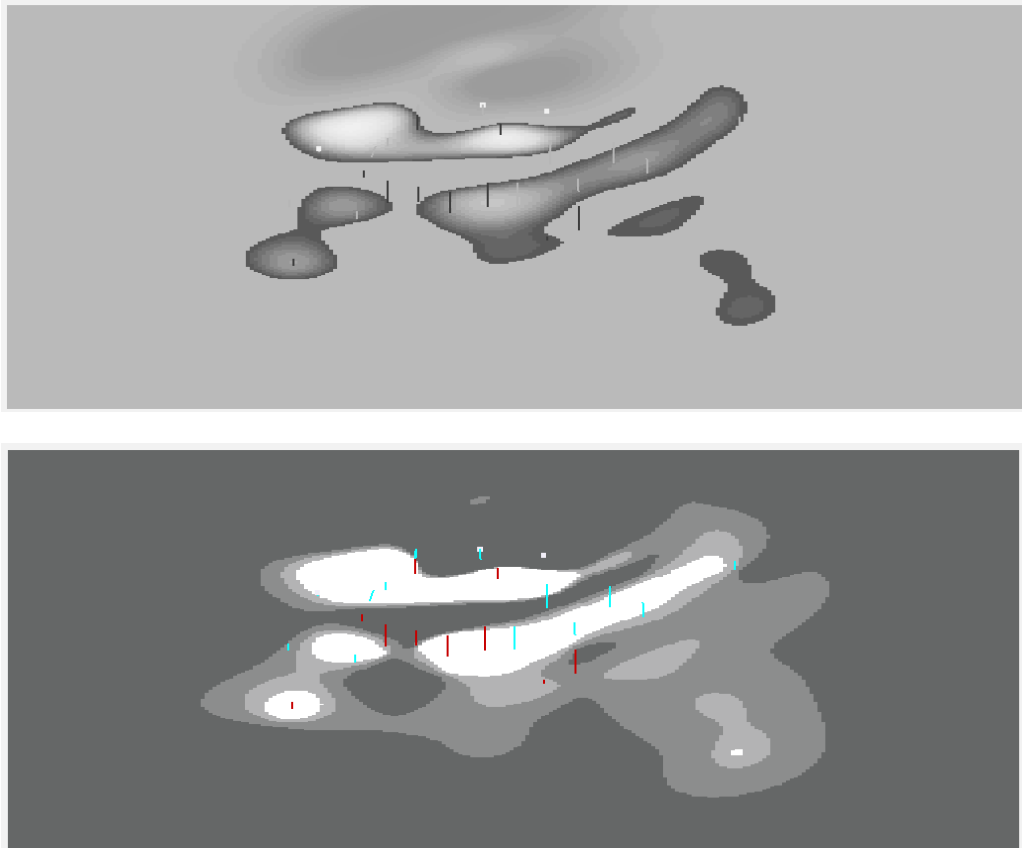
Figure 7: Vertical YOZ section with (1) top: the potential field (lower than iso-potential pale grey, above iso-potential dark grey to white) and (2) bottom: the probability to be in the domain (see text above for the color interpretation).

CONCLUSIONS

The potential field method was first applied to geological modeling when many observations can be obtained from outcrops, particularly structural data (e.g., orientation of foliation planes). The same methodology has been successfully applied to mineral deposit domaining when only exploration drill holes are available. To get an acceptable model from a geological point of view and in agreement with the data requires some heuristic iterations. For instance the variogram model cannot be easily inferred from the data that are indirectly linked to the target potential field. The input of geological knowledge (for instance regarding the plausible

anisotropy and extension of the structures) helps in making the choice. In this case, geologists fan iliar with the project and the data made expert assessments of the staged outputs to enable refinement as described in the case study above. The possibility to complement the contact points with soft data extracted from the drill holes intercepts has proved to be efficient and makes the input of somehow arbitrary data like gradients of lesser importance.

As in any cokriging approach the error variance can be obtained at any location where cokriging is performed. The probability to be in the domain can be immediately deduced from the cokriging estimate and the error variance (the potential field can be reasonably assumed Gaussian). In order to get the global uncertainty on the domain volume, conditional simulations have still to be produced.

ACKNOWLEDGEMENTS

REFERENCES

Aoki H and Matsukara Y (2008). Estimating the unconfined compressive strength of intact rocks from Equotip hardness. *Bull Eng Geol Environ, 67, 23-29*

Aug, C., Modélisation géologique 3D et caractérisation des incertitudes par la méthode du champ de potentiel. Doctoral Thesis, E.N.S. des Mines de Paris, 2004.

Calcagno, P., J.P. Chilès, G. Courrioux, and A. Guillen, Geological modeling from field data and geological knowledge. Part I. Modeling method coupling 3D potential-field interpolation and geological rules. *Physics of the Earth and Planetary Interiors*, **171(1–4)**, 2008, 147–157.

Chilès, J.P., and P. Delfiner, *Geostatistics: Modeling Spatial Uncertainty*, 2nd edition. John Wiley & Sons, New York, 2012.

Lajaunie, C., G. Courrioux, and L. Manuel, Foliation fields and 3D cartography in geology: Principles of a method based on potential interpolation. *Mathematical Geology*, **29(4)**, 1997, 571–584.

Meulenkamp F and Alvarez M (1999). Application of neural networks for the prediction of unconfined compressive strength (UCS) from Equotip hardness. *Int Jour Rock Mechanics and Min Sci, 36, 29-39*

Renard, D., J.P. Chilès, J. Rivoirard, and M. Alfaro, Assessment of the resources of a gold deposit by transitive kriging. In *Proceedings of APCOM 2013*, this volume, 2013.

Vinasco, C.J., U.G. Cordani, H. Gonzalez, M. Weber and C. Pelaez, Geochronological, isotopic, and geochemical data from Permo-Triassic granitic gneisses and granitoids of the Colombian Central Andes. *Journal of South American Earth Sciences* **21** (2006), 355-371.